**Atmospheric
Chemistry
and Physics**

Ice nucleation properties of mineral dust particles: determination of onset RH$_i$, IN active fraction, nucleation time-lag, and the effect of active sites on contact angles

G. Kulkarni[1,*] **and S. Dobbie**[1]

[1]School of Earth and Environment, University of Leeds, Leeds, UK
[*]now at: Atmospheric Science and Global Change Division, Pacific Northwest National Laboratory, Richland, WA, USA

Abstract. A newly developed ice nucleation experimental set up was used to investigate the heterogeneous ice nucleation properties of three Saharan and one Spanish dust particle samples. It was observed that the spread in the onset relative humidities with respect to ice (RH$_i$) for Saharan dust particles varied from 104% to 110%, whereas for the Spanish dust from 106% to 110%. The elemental composition analysis shows a prominent Ca feature in the Spanish dust sample which could potentially explain the differences in nucleation threshold. Although the spread in the onset RH$_i$ for the three Saharan dust samples were in agreement, the active fractions and nucleation time-lags calculated at various temperature and RH$_i$ conditions were found to differ. This could be due to the subtle variation in the elemental composition of the dust samples, and surface irregularities like steps, cracks, cavities etc. A combination of classical nucleation theory and active site theory is used to understand the importance of these surface irregularities on the nucleability parameter, contact angle that is widely used in ice cloud modeling. These calculations show that the surface irregularities can reduce the contact angle by approximately 10 degrees.

1 Introduction

Ice clouds constitute the largest source of uncertainty in predicting the Earths' climate behavior according to last Intergovernmental Panel on Climate Change 2007 report (Forster et al. 2007). The uncertainty arises in part because of the lack of understanding of the complex ways in which these clouds are formed. The dominant ice formation mechanism, for temperature below −38 °C, is homogeneous nucleation

of the supercooled water droplets and aqueous aerosol particles, with the nucleation rate increasing for colder temperatures (Jeffrey and Austin, 1997; Pruppacher and Klett, 1997; henceforth P&K97). At temperatures warmer than −38 °C ice formation take place heterogeneously. Heterogeneous ice nucleation requires special atmospheric aerosols called ice-forming nuclei (IN) which lower the free energy barrier for the nucleation and, depending upon different IN surface characteristics (e.g. size and morphology, solubility, epitaxial and active site distribution), determine the ice nucleation efficiency. Four different heterogeneous ice nucleation mechanisms are hypothesized: deposition nucleation (direct deposition of water vapor onto the surface of the IN), condensation freezing (freezing of the condensate formed on the surface of the IN), immersion freezing (freezing initiated by the IN located within the droplet), and contact freezing (freezing occurs the moment IN comes in contact with a supercooled water droplet or aerosol solution droplets). Recently Koop et al. (2000), and Jeffrey and Austin (1997) and references therein showed good agreement between homogeneous ice nucleation observations and theories. While observational and theoretical results for homogeneous nucleation can be compared with good agreement, theoretical treatments of heterogeneous nucleation that involve IN surfaces are very difficult to relate to observations (Cantrell and Heymsfield, 2005).

Past studies (DeMott et al., 2003; Cziczo et al., 2004; Richardson et al., 2007) have identified mineral dust particles as the IN inside the ice crystals collected on the ground or from clouds. Various laboratory experiments (Archuleta et al., 2005; Kanji and Abbatt, 2006; Möhler et al., 2006) have also shown that mineral dust can initiate ice formation at low saturations and warmer temperatures than homogeneous freezing, and thus can alter ice cloud properties to the larger extent than a purely homogeneous nucleation scenario. In the present experimental study not only do we

investigate mineral dust as IN, but also quantify this understanding by evaluating nucleability parameters (e.g., contact angle) which can eventually be used in cloud models.

Laboratory studies dealing with heterogeneous ice nucleation on dust particles, in particular deposition ice nucleation, have been undertaken since the 1950s. Early studies (Mason and Maybank, 1958; Roberts and Hallett 1967; Schaller and Fukuta, 1979) reported mineral dust particles as efficient IN. Recent studies (Bailey and Hallett, 2002; Archuleta et al., 2005; Salam et al., 2006; Möhler et al., 2006; Dymarska et al., 2006; Knopf and Koop, 2006; Kanji and Abbatt, 2006) have also shown that mineral dust is a good IN for various temperatures, supersaturations with respect to ice (SS_i) and sizes of dust particles. In order to better quantify the experimental heterogeneous ice nucleation rates, test nucleation theories, and further develop ice cloud parameterizations schemes it is also necessary to investigate ice nucleation as a function of time.

Few empirical heterogeneous ice formation formulations have been developed, and the commonly used ones are either SS_i dependent (Meyers et al., 1992), temperature dependent (Fletcher, 1962), or combination of both (Cotton et al., 1986). These formulations rely on data from instruments that measure ice nucleation and the formation properties at controlled temperature and saturation ratios independent of IN physical and chemical properties. The ice chamber studies for example Möhler et al. (2006) show the fractions of ice crystals formed are mainly a function of SS_i at a given temperature. However, the relative importance of temperature and SS_i on ice nucleation and the formation is not yet established. Here we have performed systematic experiments to address these questions.

Ice formation formulations in cloud models often use classical ice nucleation theory (CNT) (Comstock et al., 2008) described by P&K97. CNT in its limit, i.e. when independent of IN nature (e.g., surface characteristics), offers a reasonable estimate of ice nucleation observations. However, it fails in describing IN surface characteristics involved in the ice formation process, e.g., distribution of active sites over the IN surface. It is one of the aims of this study is to quantify the IN surface characteristics using active site theory (Gorbunov and Kakutkina, 1982) and recalculate the nucleability parameters that are used directly by CNT. In addition, the accuracy of models also relies on incorporating a broad distribution of nucleation onsets observed within a single type of IN (Knopf and Koop, 2006).

For the present study, a total of four different dust samples were collected from four different locations (three from the Saharan desert and one from Spain). The advantage of using these dust particles is that we can experiment with the natural dust particles which eliminate the variable of atmospheric processing.

In the present study, using a newly developed experimental set-up (Kulkarni et al., 2009), we have investigated the ice nucleation efficiency of natural mineral dust particles as a function of temperature, saturation ratio and nucleation time. In Sect. 2, an experimental procedure to determine various ice nucleation properties including a procedure for the ice nucleation experimental set up are presented. In Sect. 3 we present the different ice nucleation characteristics, e.g., nucleation onset as a function of temperature and saturation ratio, demonstrate the importance of active sites by measuring the nucleation time-lag, formulate a new ice cloud parameterization, and calculate the nucleability parameters used in the CNT. The conclusions are presented in Sect. 4.

2 Experimental

### 2.1 Preparation of the experimental set up

Four natural mineral dust samples were used in this study. The samples were collected at ground level from three different locations in West Africa: Nigeria, Dakar (outside the city), Dakar, during the African Monsoon Multidisciplinary Analyses campaign, and one location from Spain (South East coast). The Dakar sample collected outside the city is termed as Dakar-1 sample henceforth. The collected samples were stored and transported in inert, leak proof plastic bottles to avoid contamination. The Spanish sample was selected because it has different mineralogical elemental composition compared to West African dust samples. The collected dust samples were sieved to obtain dust particles less than 38 μm, which were then used during the experiments.

Figure 1 shows a schematic diagram of the Thermal Gradient Diffusion Chamber (TGDC) experimental apparatus. The chamber is made up of two parallel horizontal plates with the inside of both plates coated with ice. It consists of an optical microscope mounted such that the objective lens of the microscope can be raised and lowered into the optical port of the top plate. A clear glass window 2 mm thick prevents water vapor from escaping from the chamber. The experimental apparatus is housed inside a walk-in cold room, which is controlled to cool the plates of the chamber. The thickness of ice layers is maintained constant by freezing a known quantity of deionized water (18 M Ω). A detailed procedure of preparing the ice layers is outlined in Kulkarni et al. (2009). An average ice layer thickness of 4 mm was used to produce a 12 mm gap between the top and bottom ice layers. A heating mat warms the top plate and this produces a thermal and vapor diffusion gradient between the plates. Using Flatau et al. (1992), the saturation vapor pressure over the ice (e_{si}) at respective temperatures are calculated. These calculations are further used to give the relative humidity with respect to ice (RH_i) at different heights (d) for the lower half of the chamber using Eqs. (1)–(4) as follows,

$$R = d/h \tag{1}$$

$$T_d = (\Delta T \ R) + T_{bot} \tag{2}$$

$$e_{id} = \{e_{si}(T_{top}) - e_{si}(T_{bot})\} \ R + e_{si}(T_{bot}) \tag{3}$$
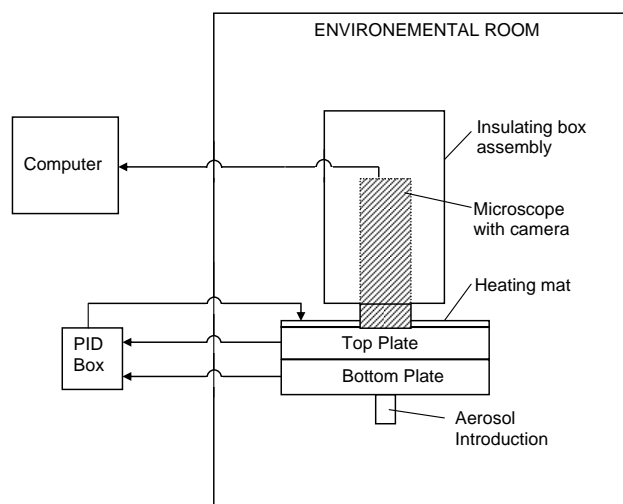
Fig. 1. Schematic diagram of the TGDC experimental set-up.

$$\mathrm{RH}_i = \{e_{id}/e_{si}(T_d)\} \cdot 100 \qquad (4)$$

where,

- h = the height between the ice layers in mm,

- ΔT = absolute difference between the top and bottom plates temperatures, $(T_{\mathrm{top}} - T_{\mathrm{bot}})$,

- $e_{si}(T_{\mathrm{top}})$ = saturation vapor pressure over ice at the top plate temperature,

- $e_{si}(T_{\mathrm{bot}})$ = saturation vapor pressure over ice at the bottom plate temperature,

- e_{id} = vapor pressure over ice at height d,

- $e_{si}(T_d)$ = saturation vapor pressure over ice at the temperature T_d.

The dust particles are deposited (refer to Kulkarni et al., 2009, for more details) onto a hydrophobic Teflon substrate affixed to the top of a sample holder rod. One end of the holder (that with the Teflon substrate) is introduced inside the chamber while the other end is connected to a micrometer. Using the micrometer the sample is raised to predetermined heights that correspond to calibrated temperatures and humidities. The technique allowed us to utilize a complete spectrum of RH_i induced inside the chamber. The uncertainty in the RH_i was calculated as follows. Initially we calculate the maximum RH_i (let us call as RH1) without considering the temperature uncertainty. Next, we calculate maximum RH_i (let us call as RH2) due to the temperature uncertainty of the plates, which is $\pm 0.4\,^\circ\mathrm{C}$. Then we subtract RH1 from RH2 to obtain the maximum RH_i uncertainty. The uncertainty obtained was less than $\pm 2.0\%$.

2.2 Procedure of ice nucleation tests

The TGDC temperature and RH_i validation was performed with direct temperature measurements as well as the phase transition of $(\mathrm{NH}_4)_2\mathrm{SO}_4$ at -19.35, -22.0 and $-28.0\,^\circ\mathrm{C}$; the accuracy of the reported values are within $\pm 2.0\%\ \mathrm{RH}_i$. Please refer to Kulkarni et al. (2009) for RH_i calibration process. The onset of ice formation is related to the temperature and RH_i conditions at which ice was first observed on any dust particle under the observation area of the microscope.

The onset RH_i of the dust particles from each location was investigated in the overall temperature range -10 to $-34\,^\circ\mathrm{C}$. In these experiments, approximately the same numbers of particles (500 per square mm) were deposited on the Teflon substrate. Each experiments had been performed on different dust particles, therefore there is no preactivation phenomenon occurring. Fresh or clean or atmospherically unprocessed dust particles are used for this study. This is because we are performing process level studies and we would like minimize any external contamination that might influence ice nucleation and the formation properties of dust particles. Also the advantage of using natural dust particles is that it eliminates the effects of cleaning/milling which is often the case with commercially available dust samples. The substrate holding the sample holder is raised to 1 mm distance above the bottom plate ice layer and the microscope is adjusted to view the dust samples. If nucleation is observed then the experiment is terminated; otherwise the sample holder is raised another 1 mm. During the experiment, optical images of the particles are recorded. The total number of dust particles counted in the field of view varies between 5 and 15, and we define the nucleation threshold as formation of ice on any 1 dust particle out of an average of 10 particles.

The active IN fraction was calculated from the fraction of ice crystal numbers observed at a given temperature and RH_i to the total number of dust particles in the field of view of the microscope. Experiments to calculate the active fraction were performed at two different temperatures ($-20\,^\circ\mathrm{C}$ and $-30\,^\circ\mathrm{C}$) and two different RH_i values (110% and 116%). In this experiment the dust particles were deposited on the Teflon substrate and the sampling rod was raised directly to the point of the desired RH_i. Images were taken from time $=0\,\mathrm{s}$ until no more new dust particles nucleated ice (time $= t_{\mathrm{max}}$). It was observed the dust particles do not nucleate immediately at time $t=0$; there was a characteristic time-lag before nucleation was observed. Once this time-lag was exceeded, the dust particles began nucleating and continued until time $= t_{\mathrm{max}}$, when no further new dust particles are activated. Knowing the number of nucleated dust particles (at time $= t_{\mathrm{max}}$) and the total number of dust particles in the observation field of view, the active IN fraction of total number of dust particles was calculated.
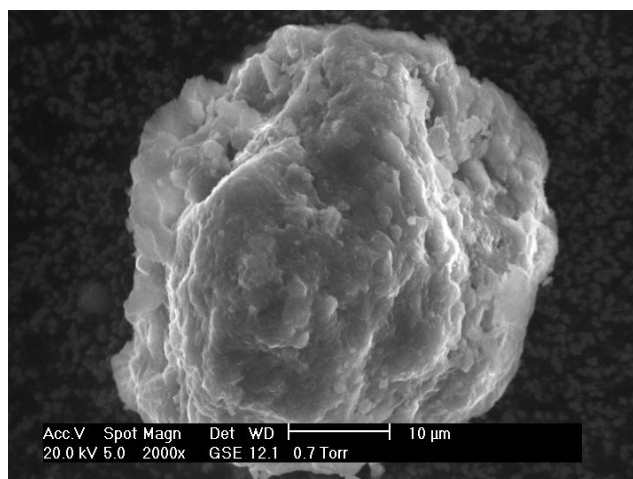
Fig. 2. Showing the high resolution scanning electron microscope image of an individual mineral dust particle from Dakar-1 source.

3 Results and discussion

3.1 Elemental analysis of dust particles

Using an Environmental Scanning Electron Microscope – Energy Dispersive X-ray (ESEM-EDX) set-up, dust particles were investigated for their morphology and elemental chemical composition. Figure 2 shows an example of the detailed surface features of a dust particle from Dakar-1 source. The irregularities of the dust surface may be due to erosion and weathering processes at the source region. Such irregularities over the surface might be responsible for the change in the surface free energy and reactivity with different chemical compounds (Kärcher and Lohmann, 2003). Foreign gases such as SO_2, NH_3 might occupy the active sites as opposed to H_2O and this can reduce the nucleability of IN (P&K97). It is also possible that irregular features, cracks, steps, or pores, might fill up with water from the vapor phase and enhance the activation of the dust particle. An interesting effect, termed to as "memory effect" or "preactivation" has been observed previously (Mason and Maybank, 1958; Roberts and Hallett, 1968; Knopf and Koop, 2006). These authors surmise that ice deposited inside the cracks might survive ice subsaturated vapor pressure conditions due to a decrease in the equilibrium vapor pressure as a result of concave curvature (also known as negative Kelvin effect). While we have not investigated these effects experimentally we have mathematically quantified the significance of these irregular features using active site theory described in the Sect. 3.5.

Ice embryo formation on the dust surface can be a selective process; a small area of the total surface can be hydrophilic and might favor the embryo formation. To minimize the uncertainties due to chemical inhomogeneity and for a greater understanding of the role of the dust surface in the ice nucleation and its formation, we determined the elemental composition of individual and bulk dust particles.

Table 1. The average weight percent of different elements in the bulk mineral dust particles collected from the four dust source regions.

Source	Atomic Percent					
Regions	% Si	% Al	% Mg	% Ca	% Na	% Fe
Dakar	47	13	3	14	5	12
Dakar-1	51	13	3	8	5	11
Nigeria	65	15	1	3	3	8
Spain	22	7	2	60	3	4

In the first examination of the dust, the elemental composition of a complete individual dust particle (larger than 10 μm) was analyzed, and later compared to the composition obtained from various small views (approximately 2×2 μm) over the same particle. In total 40 dust particles were analyzed, and a similar elemental composition distribution with ±5% variation of weight percent between the two analyses was observed. Thus it is inferred that the chemical composition over the entire dust surface is relatively homogeneous at this scale.

The second study involved bulk elemental composition analysis of 25–30 dust particles. Table 1 shows the different elements observed with their respective average weight percent distribution of Si, Al, Mg, Ca, Na and Fe. Trace amounts (<1%) of other elements, including P, K, Ti and Cl, were also observed in the analysis but are not presented. The data from Table 1 show that variations exist in the amount of elements from each source region. The similar elements for dust particles were also observed by for example, Krueger et al. (2004), Reid et al. (2003); Caquineau et al. (2002), and Glaccum and Prospero (1980). Nigerian dust has more Si but less Ca compared with the Dakar-1 and Dakar dust samples. The Dakar-1 and Dakar dust particles were also associated with a higher Fe content. Coastal dust particles have a larger percentage of Na compared with other source locations, which might be due to sea salt mixing with the dust particles. The Spanish dust had the highest percentage of Ca (60%) compared with other source locations, and this might have been derived from carbonate minerals. Variations of elemental composition of dust particles across the four source regions could be significant for ice nucleation if they are transported throughout the atmosphere. For example, from Table 1 Spanish dust is observed to contain a comparatively larger amount of calcium and dust particles containing high levels of calcium are found to be reactive with respect to nitric acid (Dentener et al., 1996). Nitrates are hygroscopic in nature and deliquesce at low relative humidity with respect to water (Tang and Fung, 1997, Al-Abadleh et al., 2003). Therefore dust particles with an abundance of calcium, once transported for long periods might be neutralized with nitric acid. These particles would then have the ability to serve
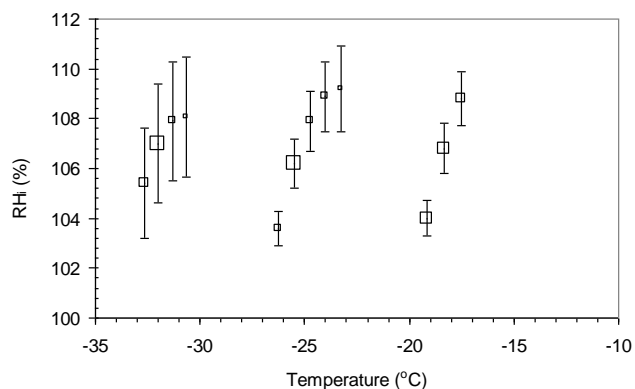
Fig. 3. Plot of onset RH_i as a function of temperature for dust samples collected from Nigeria. The data points are shown as square boxes are correlated to the frequency of nucleation events observed and error bars are less than $\pm 2.0\%$ (see text for details). Originally published in Kulkarni et al. 2009, but produced here to maintain the consistency with other onset RH_i results shown in this paper.
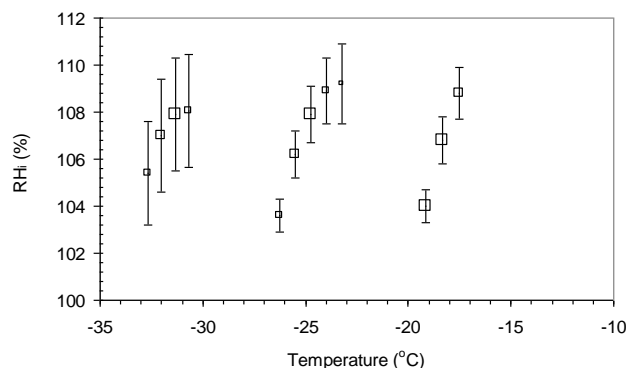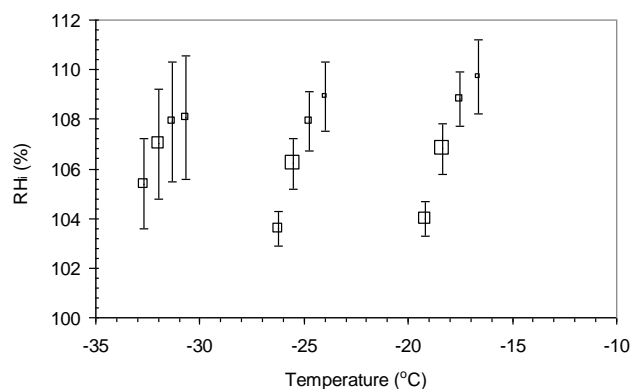

Fig. 4. Plot of onset RH_i as a function of temperature for dust samples collected from Dakar-1.

as effective IN in the appropriate atmospheric conditions. In short, dust particles provide a reactive site for many heterogeneous reactions involving many chemical species (including water vapour).

3.2 Ice onset RH_i determination

Experiments were carried out to examine the onset nucleation properties of mineral dust particles in the deposition ice nucleation mode. Figures 3 to 6 shows the plots of onset RH_i as a function of temperature for the dust samples. The data points shown as square boxes represent where onset nucleation was observed. The frequency of observing the maximum occurrences of ice formation event at that particular temperature and RH_i conditions was correlated with the size of the square box. From the size we infer that the bigger the size of the box the higher is the rate of observing the nucleation events and vice versa at those conditions. Figure 3

Fig. 5. Plot of onset RH_i as a function of temperature for dust samples collected from Dakar.

was originally published in Kulkarni et al. (2009) and is reproduced here for comparison purpose with onset RH_i results from other dust location.

It was observed that onset nucleation occurred as low as 104%, and the spread in the onset RH_i was found to vary from 104% to 110% for all the dust samples. The results are in general agreement with other past findings, even though the experimental set-up, sample preparation and types of dust particles were different. For example Mangold et al. (2005) and Knopf and Koop (2006) studied the ice nucleation abilities of Arizona test dust, and observed onset RH_i as low as 105%. In particular, our results agree with both different and similar types of dust particles including Saharan dust studied by the Kanji and Abbatt (2006). They observed that all dust samples initiated ice formation between 102 and 108% RH_i, with temperature range between $-10\,°C$ to $-55\,°C$.

Figure 6 shows the spread in the onset RH_i of Spanish dust which was found to have less of a RH_i spread than the other location dust particles. Here the range varied from 106% to 110% and this might be due to the variation in the surface chemical composition compared with the other dust particles (see Sect. 3.1 for more details) and/or the variation of surface physical features such as cracks, steps, cavities.

To test the possible effect of soluble compounds and/or bacteria, experiments were performed where we tempered the dust particles at 350 °C for 1 h. We did not find any difference between the onset RH_i determined before and after tempering. Thus we conclude that any soluble compounds and soil bacteria associated with the dust particles did not play a role during the ice nucleation experiments.

The general spread in the onset RH_i may be due to the variation in the surface characteristic features such as elemental composition inhomogeneity and distribution of active sites. But in Sect. 3.1 it is shown that dust particles have uniform elemental composition across their surface, and therefore we think this observation might not play an important role in the onset. Thus it can be inferred that the observed spread in the onset RH_i might be probably due to only a
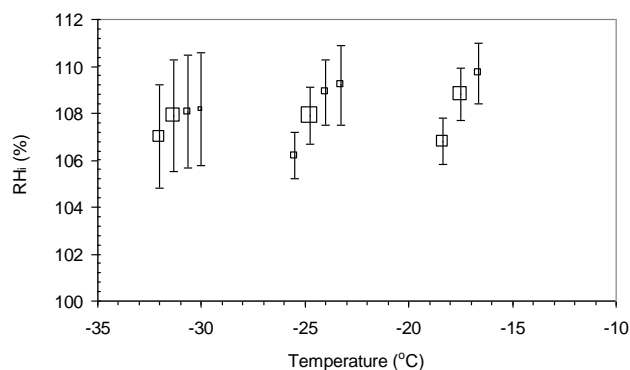
Fig. 6. Plot of onset RH_i as a function of temperature for dust samples collected from Spain.

Table 2. Comparison of mean active IN fraction (%) from two different locations. The uncertainties associated with these active fractions are less than ±20% (see text for further details).

Active IN fraction at −20 °C		
Sample	110% RH_i	116% RH_i
Dakar-1	48%	70%
Nigeria	50%	75%
Active IN fraction at −30 °C		
Sample	110% RH_i	116% RH_i
Dakar-1	22%	32%
Nigeria	32%	36%

distribution of active sites and efficiency of active sites to initiate ice nucleation varies from one dust particle to another in the same sample. Additional support for this premise comes from results shown in Sect. 3.3, the variation of nucleation time-lag.

3.3 Active fraction and nucleation time-lag

The fraction of dust particles that activate at various temperature and RH_i values are shown in Table 2. The active IN fraction increases with RH_i for the dust samples. This might be due the presence of a wide range in ice nucleation efficiencies of the dust particles within the same sample. A few dust particles might be enriched at certain efficient active sites while being depleted in another. It is still unknown what type of active sites are most effective for ice nucleation, and this has to be strong motivation for future molecular level studies to investigate these phenomena.

It is also observed that active IN fraction is higher at warmer temperature irrespective of RH_i. This might be due to the larger equilibrium ice vapor pressure at warmer temperature compared to colder temperatures. Such that the water vapor molecules at warmer temperature have high mobility, which increases the probability of water vapor molecules attaching to the dust surface.

It should be noted that the experimental RH_i values at these temperatures are well above the onset RH_i and therefore their probability of nucleation is greater than zero.

The dust from Nigeria and Dakar-1 showed a similar behavior in active IN fraction, but the percentage of active IN is higher for the sample from Nigeria compared to Dakar-1. The differences might be due to subtle variation of elemental composition across the dust surface shown in Sect. 3.1. It should be noted that the particles are exposed for longer time in IN active fraction experiments compared to onset RH_i. Then it is quite possible that some special kind of surface elemental composition might only nucleate after long time, and therefore elemental composition might play a different role

in onset RH_i and active fraction experiments. Other possible reason might be the distribution of active sites, but we do not have any experimental observations to support this idea. It is also possible there is a size dependency. Salam et al. (2006) determined the active IN fraction for kaolinite and montmorillonite dust particles. They calculated active IN fraction from the ratio of the ice crystal number concentration active at a given temperature over the total number of ice crystals at 100% relative humidity with respect to water at −40 °C, and observed increasing active IN fraction with increase in RH_i. We note a similar trend. Their results showed that montmorillonite particles have a higher active IN fraction at −20 and −30 °C compared to kaolinite. Other possible reasons to obtain higher IN active fraction could be: use of larger size particles, small number of particles and the exposure time. It should be noted that in the IN fraction calculations the experiment is terminated when no further ice formation events are observed.

The importance of active sites in the deposition ice nucleation mode can be further investigated by understanding the "nucleation time-lag". An appreciable time delay was observed for the appearance of the first ice cluster on any individual dust particle in the field of view ($125\,\mu m \times 94\,\mu m$), once the dust particles has been exposed to different temperature and RH_i conditions. The time delay at −30 °C is longer compared to −20 °C at two different RH_i conditions for Dakar-1 location dust particles.

To date, only one study (Anderson and Hallett, 1976) has been conducted to understand time-lag of ice formation on AgI and CuS surfaces as a function of temperature and RH_i. The present work is the first of its type to study the nucleation time-lag of Saharan mineral dust particles at various constant temperature and RH_i values for deposition mode ice nucleation. Anderson and Hallett (1976) observed the time-lag is longest at low RH_i. They observed time lag of 30 to 300 s at −5 °C and 103% temperature and RH_i respectively. Experiments at −23.8 °C and 115% temperature and

RH_i respectively they observed time lag of 3 to 20 s. Time lag was observed to be longer at lower RH_i. This is in agreement with the present experiments, where it is observed that the lag is longer at 110% compared with 116% RH_i by approximately 40 s. We observe at 110% RH_i the time-lag, at $-30\,°C$ and $-20\,°C$, is between 80 to 170 s and 85 to 135 s, respectively; whereas, at 116% RH_i it is between 85 to 120 s and 65 to 100 s, respectively. It is observed that the nucleation experiments performed at low temperature and RH_i values require more time for ice formation. We note that at 110% RH_i the lower limit time-lag at warmer temperature is higher. It is possible that at 110% RH_i the vapor density might be low enough such that there is no influence of temperature on the time-lags. However, these hypothesis needs to be investigated in the future experiments.

The time delay suggests variation of active sites within the dust particles. According to P&K (1997), each active site on any individual dust surface requires a critical RH_i, at a given temperature, which must be applied for a critical length of time for an ice embryo to form and to grow to an ice cluster, and an eventual ice crystal. The time delay for the ice embryo formation can also be associated with the time required to overcome the free energy barrier for nucleation. It should be noted that nucleation time-lag experiments were conducted at RH_i higher than the threshold RH_i (onset RH_i) at respective temperatures. The maximum energy barrier value can be given by Mason (1971) Eq. (1),

$$\Delta G = \frac{4}{3}\,\pi\,\sigma\,r^{*2} \tag{5}$$

Where σ is the surface tension, and r^* is the critical radius of the ice embryo given as Eq. (6),

$$r^* = \frac{2\,\sigma\,M}{\rho\,R\,T\,\ln{(e/e_s)}} \tag{6}$$

where M is the molecular weight of water vapor, ρ is the ice density, R is universal gas constant, T is the temperature, e is the equilibrium vapor pressure, and e_s is the saturation vapor pressure.

Assuming $r^* = 0.01\,\mu m$ (P&K 1997) we calculated using Maxwell diffusion growth theory the time required for the ice embryo to grow a size (=1.1 μm) detectable by the microscope. It was found that the time required for an embryo to grow to this size is 36 s at $-20\,°C$ and 110% RH_i. This suggests that the if the total time observed is 85 s then time required for the establishment of ice embryo had taken approximately 49 s, which is the time needed to overcome the energy barrier imposed by the dust surface. Due to various uncertainties, e.g. resolution of the microscope (1.1 μm), assumption of the initial size of the ice embryo (0.01 μm in diameter), neglecting condensational kinetic corrections (latent heat and ventilation effects), time required by the particles to equilibrate with the surrounding, these calculations involving the time required to overcome the free energy barrier should

be regarded as upper estimations. However, these uncertainties should be in the order of few seconds. For example, it was calculated that it takes approximately 3.3 s for a dust particle of size 20 μm to reach the equilibrium temperature of $-30\,°C$. Therefore we can say that comparatively nucleation time-lag times are much longer and the particles are not being influenced by non-equilibrium conditions. Developing ice nucleation parameterizations as a function of free energy barrier and nucleation time-lag can be one of the solutions to represent the complex nature of heterogeneous ice nucleation in global climate models. Future work should be carried out to gain a better understanding about the type of active sites that may increase or decrease the energy barrier. This might help in understanding why sometimes the aerosol particles do not participate in ice nucleation processes under favorable atmospheric conditions.

3.4 Rate of ice crystal formation as a function of time

Figure 7 shows the fraction of aerosols activated plotted as a ratio of number of ice crystals (Ni) observed to the total number of IN (Nf), as a function of time (t) for the two different geographical locations, Dakar-1 and Nigeria. Total 60 experiments (each experiment had 5 to 10 particles and different particles in every experiment) were carried out to obtain the data points. An approximate behavior for the ice crystal formation can be represented as Eq. (7),

$$F_i = 1.0128\,(1 - \exp(-B\,t)) \tag{7}$$

Where $F_i = $ Ni/Nf and $B = 111.33$.

Figure 7 shows that the dust particles from at least these two sources have the unique ability to initiate ice formation in the early time period of ice cloud development. The wide scatter in the data shown in the Fig. 7 can be attributed to the following two reasons. One, subtle variation in the dust surface elemental composition. Recently Eastwood et al. (2008) showed in their ice nucleation experiments that dust minerals with different elemental composition have a wide range of onset nucleation RH_i. Minerals like Quartz (SiO_2) and Calcite ($CaCO_3$) were observed to be nucleating at higher RH_i compared to Kaolinite ($Al_4Si_4O_{10}(OH)_8$) and Montmorillonite ($(Na,Ca)_{0.3}(Al,Mg)_6(Si_4O_{10})_3(OH)_6$-$nH_2O$). The montmorillonite has more $-OH$ groups compared to Kaolinite, and the variation might enhance the nucleation as $-OH$ groups in former mineral can attract more water vapor molecules (Salam et al., 2006). Shown in Table 1 are the elemental composition of the dust particles from Dakar-1 and Nigeria. There are subtle variations in the elemental composition, and this might affect the total number of IN at any particular temperature and RH_i condition.

The second reason would be the variation of surface irregularities or roughness across the dust particles from both the locations. These surface features can be viewed as the wide distribution of active sites having different free energies of interaction with water molecules. This energetically
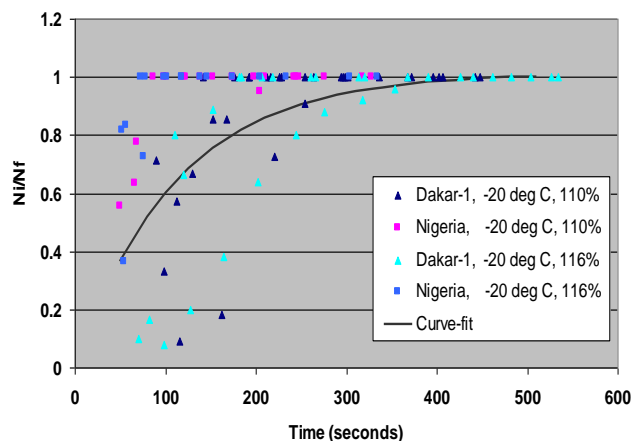
Fig. 7. The ratio of number of ice crystals formed in time t for various dust particles. Triangles and squares on the graph indicate the dust particles from Dakar-1 and Nigeria, respectively. Legend format shown is figure symbol, location of dust source, temperature and RH_i. Best exponential type fit is shown as a curve-fit, which follows the experimental data from both the locations.

non uniform distribution of active sites, gives each site a different probability of becoming an active ice-nucleating site (Rosinski, 1980). It can be hypothesized that Dakar-1 location might have surface features different than Nigeria, and all dust particles at each location have nearly similar surface features. The mineralogy specific to a location as well as the local weathering and erosion characteristics might lead to this unique surface pattern. The ESEM images of these dust particles were analyzed to identify these patterns, but just visual inspection of the images did not reveal any patterns. More in-depth image analysis at very high resolution of nanometer scale, including accurately measuring the particle surface area, needs to be carried out to understand more details about the surface patterns.

Furthermore Eq. (7) is modified to obtain rate of ice crystal formation (D_{nice}/dt) as a function of total number of aerosol particles (n_p) and time (t) given as Eq. (8),

$$D_{nice}/dt = n_p \, K \, \exp(-C \, t) \tag{8}$$

where K=112.755 and C=111.33 are the constants, and suffix "p" indicates the particle.

The above developed parameterization scheme can be used in the process level ice nucleation studies, which deals with the individual aerosol-cloud interactions. To better understand the effect of dust particles on large-scale cloud properties these process level studies are very useful. Recently, Baker and Peter (2008) highlighted the importance of such studies to predict the development of individual clouds and cloud systems. It should be also noted these simple schemes Eqs. (7) and (8) lack the information such as dust particle surface area, chemistry and are independent of RH_i. These schemes need to be tested in cloud models and requires
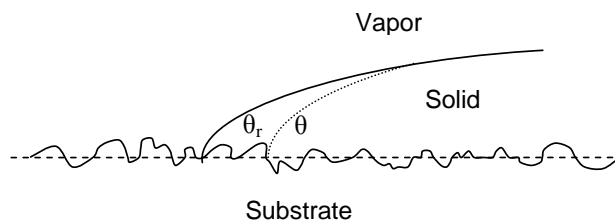
Fig. 8. Schematic showing the definitions of contact angle and contact line. θ and θ_r are the contact angles when the substrate is smooth and rough, respectively. θ_r is less than θ because of the surface irregularities of the substrate.

further improvement. Future research should be carried out extending these studies to different types of dust particles at various temperature and RH_i conditions and characterizing the source locations and aging and transport.

3.5 Contact angle and active site theory

In addition to developing the new ice cloud parameterizations schemes, the results are adapted to improve existing schemes and to suggest the new values for the various variables/parameters involved in the schemes. One common scheme used in the ice cloud modeling studies (Comstock et al., 2008) is the classical nucleation theory (P&K97, 341–345 pp.). The nucleation rate calculated by this theory is as Eq. (9),

$$J = E_o \exp\{-(\frac{\Delta G_o}{kT} \, f(m) - \frac{A(1-m)\sigma}{kT})\} \tag{9}$$

where J is the nucleation rate ($cm^{-2} \, s^{-1}$) and J = N/($S_A \, t$), N is the number of ice particles observed in time t, S_A is the surface area of the particles determined using Martin's diameter (Hinds, 1982), E_o is the pre-exponential factor ($cm^{-2} \, s^{-1}$), ΔG_o is the activation energy barrier for homogeneous nucleation, k is the Boltzmann constant, T is the temperature, A is the surface area having active sites or defect area, f(m) is $(2+m)(1-m)^2/4$, and m is defined as $cos(\theta)$ with θ being the contact angle. Table 3 tabulates the range of J values at different temperature and RH_i conditions.

The ice forming ability of IN can be expressed in terms of θ between the dust surface and an ice embryo using Young's relation defined as Eq. (10), and shown in Fig. 8,

$$m = cos(\theta) = (\sigma_{CV} - \sigma_{CS})/\sigma_{SV} \tag{10}$$

Where m is the wettability parameter, σ_{ij} are surface free energies, and subscripts C, V and S refers to catalyzing substrate (dust surface in the present study), vapor (water vapor) and solid (ice) respectively.

The contact line of an ice-embryo growing upon a smooth solid substrate surface is a dashed line shown in Fig. 8. In reality the substrate has a degree of roughness and this decreases the θ to a new contact angle specified as θ_r. The

Table 3. Range of experimental heterogeneous nucleation rates (J) and contact angles (θ) at two different temperature and RH$_i$ values for the dust samples from Dakar-1 and Nigeria.

Contact angle at $-20\,^\circ$C				
Sample	110% RH$_i$		116% RH$_i$	
	J	θ	J	θ
Dakar-1	25–173	15.5–15.9	53–143	19.5–19.9
Nigeria	51–480	15.4–15.8	90–389	19.4–19.6
Contact angle at $-30\,^\circ$C				
Sample	110% RH$_i$		116% RH$_i$	
	J	θ	J	θ
Dakar-1	18–197	15.1–15.3	28–324	19.0–18.9
Nigeria	47–425	15.0–15.1	81–490	18.8–18.9

rough substrate can be assumed to possess the active sites in the form of steps, cavities etc. To understand the effectiveness of active sites on the ice forming ability of IN, we initially calculate the contact angle without including the active sites (by substituting $A=0.0$ in Eq. 9). Table 3 tabulates the contact angle determined for two dust source locations, and it can be observed that the contact angle varies approximately between 15 to 20 degrees for 110% and 116% RH$_i$ respectively.

To understand the influence of active sites on the contact angle, we first estimate the fraction (F) of the total surface area which consist of active sites, and then using dust particle surface area (A_s) we calculated the defect area (A) ($A = F\times A_s$). Then substituting A into Eq. (9) and using the same experimental nucleation rate, we re-calculate the contact angles. The following Eqs. (11) and (12) are used to calculate F (Fletcher, 1969; Gorbunov and Kakutkina, 1982; Han et al., 2002, and references therein),

$$P = 1 - \exp[-A_s \int_{A_o}^{s} n(S)\, S\, dS], \qquad (11)$$

where

$$n(S) = \text{F}\, A_o^{-2} \exp\{-\gamma^2 [\ln(S/A_o)]^2\}, \qquad (12)$$

where A_o is the minimum area of one active site ($=2$e - $15\,\text{cm}^2$) (Fletcher, 1969), S is the surface area of one active site ($=2\times A_o$), γ is the width of active site distribution ($=1$), A_s is the surface area of aerosol particle ($=1\,\mu$m in radius). We assume $1\,\mu$m size because this size is widely observed (Jickells et al., 2005; Hoornaert et al., 2003; Ginoux et al., 2001) and used in the models. At present we do not know how active sites influence the ice nucleation efficiency under different temperature and RH$_i$ conditions, and therefore

Table 4. Range of experimental heterogeneous nucleation rates (J) and contact angles (θ) at two different temperature and RH$_i$ values for the dust samples from Dakar-1 and Nigeria.

	Contact angle (θ)
Without active surface area ($A=0.0$)	15.1 degrees
With active surface area ($A=9$e-$07\times A_s$)	5.1 degrees

we assume half probability ($P=0.5$) distribution (Heneghan and Haymet, 2002) and solving the Eqs. (11) and (12) gives F=9e-07.

The calculated A is substituted into Eq. (9) to re-calculate the revised contact angle. Table 4 tabulates the change in contact angle after including the effect of active surface in the calculation.

The tabulated values in Table 4 illustrate the effect of inclusion of active surface on the contact angle. The revised contact angle value is approximately 10 degrees less than the values when active surface areas are not considered. It is known that the lower the contact angle of the aerosol particle the higher the nucleation efficiency. Generally in ice cloud modeling studies the nucleation rates are calculated by assuming a constant contact angle over the smooth aerosol particle. Use of revised contact angles may impact these modeling results (Comstock et al., 2008; Liu and Penner, 2005).

4 Conclusions

Ice nucleation properties (i.e. the onset RH$_i$, active fraction, and nucleation time-lag) of mineral dust particles collected from the Sahara and Spain were determined using a TGDC experimental set-up. Using these measurements two parameterization studies were undertaken: the rate of ice crystal formation as a function of time and a calculation of nucleation parameters (contact angles) using active site theory.

The onset RH$_i$ results show that dust particles nucleate at values as low as 104%. This may be due to the use of large dust particles ($>1\,\mu$m diameter which is normally observed); the large size may result in at least one favorable nucleation site per particle which was active at low RH$_i$. The spread observed in onset RH$_i$ was from 104% to 110%. The spread for Spanish dust was from 106% to 110%, which is narrow compared to Saharan dust. Neglecting the experimental uncertainty the requirement of higher RH$_i$ compared to Saharan dust particles may be due to the presence of Ca-containing minerals, and further supports the evidence that Ca-dominant minerals such as quartz or calcite are poor ice nuclei.

The total active IN fraction of dust particles from two different source regions, Dakar-1 and Nigeria, was determined. Higher fractions were observed at higher RH$_i$. This may be explained by the fact that dust particles may posses a

distribution of active sites, each requiring a different onset RH$_i$ to activate. This premise further supports the nucleation time-lag measurements. The total time-lag observed for these dust particles varied from 65 to 170 s. These measurements are further used to estimate the time required for the ice embryo formation. Our calculation shows at $-20\,°C$ and 110 RH$_i$, the time required is approximately 49 s. Due to various experimental uncertainties these calculations should be regarded as upper estimations. Future studies are needed to reduce these uncertainties and determine the microphysical properties for a complete understanding of ice nucleation and the formation on IN.

It is observed that the IN fraction increases with time showing very little dependency on the RH$_i$. An empirical fit is suggested, which is further modified to provide a new parameterization for the rate of ice crystal formation as a function of time at variable temperature and RH$_i$. This parameterization may be useful for determining the initial ice particle concentration in ice clouds for studies involving the evolution or the initial phase of cloud formation. It is noted that the empirical fit equation does not describe all of the data, and thus we believe new parameterization should be explored in future studies.

To understand the effect of surface roughness on the ice forming ability of a dust surface we make use of CNT. By using experimental heterogeneous nucleation rates in conjunction with CNT we have determined the contact angles between an ice embryo and the dust surface. The range of contact angles is found to vary from 15 to 20 degrees. These results are used in conjunction with a theoretical model to evaluate the significance of active sites (measured in terms of percentage of surface roughness area) on the contact angle. The revised contact angle values are approximately 10 degrees less than the values when active surface roughness areas are not considered.

This study has demonstrated that laboratory measurement data can be successfully utilized to develop ice cloud parameterizations and estimate the range of nucleability parameters involved in existing parameterizations schemes. These measurements may help to develop and evaluate models dealing with aerosol cloud interactions or process level studies, which are necessary for understanding the impact of ice on climate. For a complete understanding of ice nucleation processes, more laboratory studies of this kind are urgently required to address the need to better resolve the impacts of ice on climate.

Edited by: T. Koop

References

Al-Abadleh, H. A., Krueger, B. J., Ross, J. L., and Grassian, V. H.: Phase transitions in calcium nitrate thin films, Chem. Commun., 2796–2797, 2003.

Anderson, B. J. and Hallett, J.: Supersaturation and time dependence of ice nucleation from the vapor on single crystal substrates, J. Atmos. Sci., 33, 822–832, 1976.

Archuleta, C. M., DeMott, P. J., and Kreidenweis, S. M.: Ice nucleation by surrogates for atmospheric mineral dust and mineral dust/sulfate particles at cirrus temperatures, Atmos. Chem. Phys., 5, 2617–2634, 2005,
http://www.atmos-chem-phys.net/5/2617/2005/.

Bailey, M. and Hallett, J.: Nucleation effects on the habit of vapour grown ice crystals from -18 to $-42°C$, Q. J. Roy. Meteor. Soc., 128, 1461–1483, 2002. .

Baker, M. B. and Peter, T.: Small-scale cloud processes and climate, Nature, 451, 299–300, 2008.

Cantrell, W. and Heymsfield, A.: Production of ice in tropospheric clouds – A review, B. Am. Meteorol. Soc., 86(2), 795, 2005.

Caquineau, S., Gaudichet, A., Gomes, L., and Legrand, M.: Mineralogy of Saharan dust transported over northwestern tropical Atlantic ocean in relation to source regions, J. Geophy. Res., 107(D15), 4251, doi:10.1029/2000JD000247, 2002.

Cziczo, D. J., Murphy, D. M., Hudson, P. K., and Thomson, D. S.: Single particle measurements of the chemical composition of cirrus ice residue during CRYSTAL-FACE, J. Geophys. Res., 109, D04201, doi:10.1029/2003JD004032, 2004.

Comstock, J. M., Lin, R. F., Starr, D. O., and Yang. P.: Understanding Ice Supersaturation, Particle Growth, and Number Concentration in Cirrus Clouds, J. Geophys. Res., 113, D23211, doi:10.1029/2008JD010332, 2008.

Cotton, W. R., Tripoli, G. J., Rauber, R. M., and Mulvihill, E. A.: Numerical simulation of the effects of varying ice crystal nucleation rates and aggregation processes on orographic snow fall, J. Clim. Appl. Meteorol., 25, 1658–1680, 1986.

DeMott, P. J., Sassen, K., Poellot, M. R., Baumgardner, D., Rogers, D. C., Brooks, S. D., Prenni, A. J., and Kreidenweis, S. M.: African dust aerosols as atmospheric ice nuclei, Geophys. Res. Lett., 30(14), 1732, 2003.

Dentener, F., Carmichael, G., Zhang, Y., Crutzen, P., and Lelifeld, J.: The role of mineral aerosols as a reactive surface in the global troposphere, J. Geophys. Res., 101, 22869–22890, 1996.

Dymarska, M., Murray, B. J., Sun, L., Eastwood, M. L., Knopf, D. A., and Bertram, A. K.: Deposition ice nucleation on soot at temperatures relevant for the lower troposphere, J. Geophys. Res., 111, D04204, doi:10.1029/2005JD006627, 2006.

Eastwood, M. L., Cremel, S., Gehrke, C., Girard, E., and Bertram, A. K.: Ice nucleation on mineral dust particles: Onset conditions, nucleation rates and contact angles, J. Geophys. Res., 113, D22203, doi:10.1029/2008JD010639, 2008.

Flatau, P. J., Walko, R. L., and Cotton, W. R.: Polynomial fits to Saturation Vapor Pressure, J. Appl. Meteorol., 31, 1507–1513, 1992.

Fletcher, N. H.: Physics of Rainclouds, Cambridge University Press, Cambridge, 1962.

Fletcher, N. H.: Active sites, and ice crystal nucleation, J. Atmos. Sci., 26, 1266–1271, 1969.

Forster, P., et al.: Climate Change 2007: The Physical Science Basis. Contribution of Working Group I to the Fourth Assessment

Report of the Intergovernmental Panel on Climate Change, Cambridge 10 University Press, Cambridge, UK and New York, USA, 2007.

Gerbunov, B. and Kakutkina, N.: Ice crystal formation on aerosol particles with a non-uniform surface, J. Aerosol Sci., 13, 21–28, 1982.

Ginoux, P., Chin, M., Tegen, I., et al.: Sources and Distributions of Dust Aerosols Simulated with the GOCART Model, J. Geophy. Res., 106(D17), 20255–20273, 2001.

Glaccum, R. A. and Prospero, J. M.: Saharan aerosols over the tropical north Atlantic – mineralogy, Mar. Geol., 37, 295–321, 1980.

Han, J. H., Hung, H. M., and Martin, S. T.: Size effect of hematite and corundum inclusions on the efflorescence relative humidities of aqueous ammonium nitrate particles, J. Geophys. Res., 107(D10), 4086, doi:10.1029/2001JD001054, 2002.

Heneghan, A. F. and Haymet, A. D. J.: Liquid-to-crystal nucleation: A new generation lag-time apparatus, J. Chem. Phys., 117, 5319, 2002.

Hinds, W. C.: Aerosol technology – properties, behavior, and measurement of airborne particles, Wiley publications, 1982.

Hoornaert, S., Godoi, R. H. M., and Van Grieken, R.: Single particle characterisation of the aerosol in the marine boundary layer and free troposphere over Tenerife, NE Atlantic, during ACE-2, J. Atmos. Chem., 46(3), 271–293, 2003.

Jeffery, C. A. and Austin, P. H.: Homogeneous nucleation of supercooled water: Results from a new equation of state, J. Geophys. Res., 102(D21), 25269–25280, 1997.

Jickells, T. D., An, Z. S., Andersen, K. K. et al.: Global Iron Connections between Desert Dust, Ocean Biogeochemistry, and Climate, Science, 308(5718), 67–71, 2005.

Kanji, Z. A. and Abbatt, J. P. D.: Laboratory studies of ice formation via deposition mode nucleation onto mineral dust and n-hexane soot samples, J. Geophys. Res., 111, D16204, doi:10.1029/2005JD006766, 2006.

Kärcher, B. and Lohmann, U.: A parameterization of cirrus cloud formation: Heterogeneous freezing, J. Geophys. Res., 108, 4402, 2003.

Knopf, D. A. and Koop, T.: Heterogeneous nucleation of ice on surrogates of mineral dust, J. Geophys. Res., 111, D12201, doi:10.1029/2005JD006894, 2006.

Koop, T., Luo, B., Tsias, A., and Peter, T.: Water activity as the determinant for homogeneous ice nucleation in aqueous solutions, Nature, 406, 611–614, 2000.

Krueger, B. J., Grassian, V. H., Cowin, J. P., and Laskin, A.: Heterogeneous chemistry of individual mineral dust particles from different dust source regions: the importance of particle mineralogy, Atmos. Environ., 38, 6253–6261, 2004.

Kulkarni, G., Dobbie, S., and McQuaid, J. B.: A new thermal gradient ice nucleation diffusion chamber instrument: design, development and first results using Saharan mineral dust, Atmos. Meas. Tech., 2, 221–229, 2009,
http://www.atmos-meas-tech.net/2/221/2009/.

Liu, X. and Penner, J. E.: Ice nucleation parameterization for global models, Meteorol. Z., 14, 499–514, 2005.

Mangold, A., Wagner, R., Saathoff, H., et al.: Experimental investigation of ice nucleation by different types of aerosols in the aerosol chamber AIDA: implications to microphysics of cirrus clouds, Meteorol. Z., 14(4), 485–497, 2005

Mason, B. J. and Maybank, J.: Ice nucleating properties of some natural mineral dusts, Q. J. Roy. Meteor. Soc., 84, 235–241, 1958.

Mason, B. J.: The Physics of Clouds, Oxford: Clarendon Press, 1971.

Meyers, M. P., DeMott, P. J., and Cotton, W. R.: New primary ice nucleation parameterization in an explicit cloud model, J. Appl. Meteorol., 31, 708–721, 1992.

Möhler, O., Field, P. R., Connolly, P., Benz, S., Saathoff, H., Schnaiter, M., Wagner, R., Cotton, R., Krämer, M., Mangold, A., and Heymsfield, A. J.: Efficiency of the deposition mode ice nucleation on mineral dust particles, Atmos. Chem. Phys., 6, 3007–3021, 2006,
http://www.atmos-chem-phys.net/6/3007/2006/.

Phillips, V. T. J., DeMott, P. J., and Andronache, C.: An Empirical Parameterization of Heterogeneous Ice Nucleation for Multiple Chemical Species of Aerosol, J. Atmos. Sci., 65, 2757–2783, 2008.

Pruppacher, H. R. and Klett, J. D.: Microphysics of Clouds and Precipitation, Springer Publications, New York, 1997.

Reid, E. A., Reid, J. S., Meier, M. M., et al.: Characterization of African dust transported to Puerto Rico by individual particle and size segregated bulk analysis, J. Geophys. Res. 108(D19), 8591, 2003.

Richardson, M. S., DeMott, P. J., Kreidenweis, S. M., et al.: Measurements of heterogeneous ice nuclei in the Western US in springtime and their relation to aerosol characteristics, J. Geophys. Res., 112(D2), D02209, doi:10.1029/2006JD007500, 2007.

Roberts, P. and Hallett, J.: A laboratory study of the ice nucleation properties of some mineral particulates, Q. J. Roy. Meteor. Soc., 94, 25–34, 1967.

Rosinski, J.: Heterogeneous nucleation of ice on surfaces of liquids, J. Phys. Chem., 84(14), 1829–1832, 1980.

Salam, A., Lohmann, U., Crenna, B., Lesins, G., Klages, P., Rogers, D., Irani, R., MacGillivray, A., and Coffin, M.: Ice nucleation studies of mineral dust particles with a new continuous flow diffusion chamber, Aerosol Sci. Tech., 40(2), 134–143, 2006.

Schaller, R. C. and Fukuta, N.: Ice nucleation by aerosol particles: Experimental studies using a wedge-shaped ice thermal diffusion chamber, J. Atmos. Sci., 36, 1788–1802, 1979.

Tang, I. N. and Fung, K. H.: Hydration and Raman scattering studies of levitated microparticles $Ba(NO_3)_2$, $Sr(NO_3)_2$, and $Ca(NO_3)_2$, J. Chem. Phys., 106, 1653–1660, 1997.